Harmonic Evaluation of Z-Source PWM Inverter for Wind Powered Industrial Drive Applications

Max Savio[1] and Sasikumar Murugesan[2]

[1]Department of Electrical and Electronics Engineering,
Jeppiaar Institute of Technology, Chennai, India
[2]Department of Electrical and Electronics Engineering,
Jeppiaar Engineering College, Chennai, India.

Abstract: In this paper, a comparison on Total Harmonic Distortion (THD) by using different pulse width modulation schemes for an industrial drive application is performed. The induction motor drive system driven by a wind energy conversion system is modeled using a Self-Excited Induction Generator. To obtain a constant frequency output an Impedance Source Inverter (ZSI) is connected between the source and the load. The ZSI is selected to avoid the shoot-through limitation which is observed in other conventional PWM inverters. The PWM switching techniques like Trapezoidal PWM, Sinusoidal PWM and Space Vector PWM techniques are mathematically modeled operating at a switching frequency of 10 kHz to control the induction motor drive system though pulse generation. The proposed method is simulated using MATLAB program and the current harmonic levels for driving the IM drive are analyzed. The comparative analysis of current harmonics illustrates the efficient implementation of PWM technique for the drive applications. Based on the simulation evaluation a similar hardware prototype model is setup for a 900W system using Space Vector PWM technique and the results are compared.

Keywords: Harmonic Distortions, Pulse Width Modulation (PWM), Induction Motor (IM), Wind Power.

1. Introduction

The practical implementation of Self-Excited Induction Generator is more commonly used in the field of wind energy conversion system for its mechanical and electrical characteristics with more effectiveness [1]. The investigation studies on various characteristics of SEIG have proved that the conversion system is dynamically more effective. The applications can differ on various needs. The research on gird connections for the optimum utilization using wind power is predominantly emerging for industrial applications [2]-[3]. However the practical implementations have proved that the use of Self-Excited Induction Generator as the wind power source contributing effectively and which is practically validated [4]. In industrial applications the source is sensitive to the load requirements. A balanced load conditions have no major effect on the source distributing the power to the grid utility. Any unbalanced load causing disturbances in the power lines probably affects the system causing over voltages, surges, swell and sag. It is the most important issues in any industrial applications where such effects have to be removed or reduced to the level of standard requirement. Induction Generators used for power generation can probably experience temporary over voltage problems [5]-[6].

In concentration to the above problems fixed speed wind energy conversion system also requires power electronic circuits operating at optimized effective conditions with constant voltage and frequency. The power electronic circuits are being used to convert the sources either from AC to DC or DC to AC based on its application. The requirements of a three phase industrial drive are constant voltage and frequency. Conversion AC-AC can be done directly or

Received: November 16th, 2013. Accepted: February 26th, 2014

indirectly by converting to DC and then to AC. A simple three phase inverter converting from DC to AC experiences shoot-through problem during switching operation is eliminated using impedance sources connected across a normal inverter. This eliminated the shoot-though problem [7]. The inverter switching techniques are comparatively more important to the of inverter selection. The power conversion from DC to AC applied to induction motor drives must have low harmonic levels to reduce the power loss. Use of filters at the output levels for each application will practically increase the cost and size of the system. To function effectively any inverter can be switched using the possible switching techniques. The sinusoidal pulse width modulation (SPWM) is one of the commonly practice technique used in single and three phase inverters. The PWM techniques have used different carrier waves to generate the pulses effectively [8]. The use of SPWM in case of AC to AC converter has been effective in implementation [9]. Similarly the dead time compensation in inverter operation is concentrated in the industrial applications. The industrial motors operated using effective control topology is estimated in real time basis which is found effective [10]-[11]. Since it becomes the issue of harmonic occurrence in industrial applications it is necessary to select an effective technique of switching topology. Many three phase inverters are controlled using the Space Vector Pulse Width Modulation (SVPWM) for better outputs with minimized harmonic levels. The modeling of SVPWM for single impedance network in a three level inverter is discussed [15]-[16]. The industrial motors have a wide range of applications. The three phase induction motors are sensitive to system level power losses when various control techniques are used to operate it. To perform better output, the motors are designed to operate at wide range and of frequency with high accuracy [17]-[18].

The work performed in this paper discusses about various inverter switching topologies and shows the comparison of total harmonic distortion (THD) for an industrial motor applied at constant loaded conditions. This comparative analysis is performed for an inverter which is powered using the wind driven self-excited induction generator modeled with a real time implementation assumptions [12]. The proposed system design in shown in the figure 1.

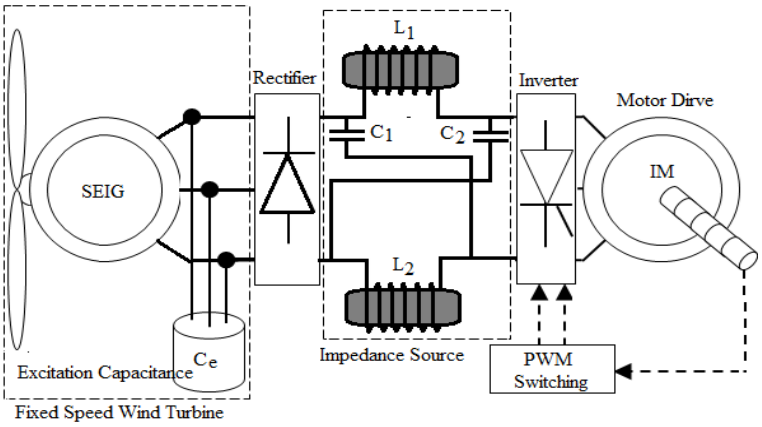

Figure 1. Block Diagram of the Proposed System

The SEIG is modeled with the machine variables of the induction generator (IG) with excitation capacitance (Ce) connected in shunt to operate with self-excitation producing the output proportional to the wind velocity and other turbine parameters. The output is rectified using bridge rectifier and then given to impedance source inverter (ZSI) which is the impedance source (L and C) connected to the input of the inverter. An Induction Motor (IM) drive is connected at the output of the inverter terminals. The drive outputs of rotor speed (ω_e) and the torque (T) are used to control the drive applications by producing optimum switching pulses. The switching pulses are tested with Trapezoidal PWM (TPWM), Sinusoidal PWM (SPWM) and Space Vector PWM (SVPWM) at a switching frequency of 10 kHz.

2. Modeling of Wind Driven SEIG

The modeling of Self-Excited Induction Generator (SEIG) is performed using the three phase induction generator machine equations. The SEIG modeling is essentially the performance of an induction motor driven by a prime mover. The prime mover here considered refers to the practical wind impact concept on blade theory. The prime mover excitation is obtained by connecting capacitor at the stator terminals. The capacitor which excites the output is referred as excitation capacitance (C_e). The excitation capacitance value is selected by performing suitable test and the maximum and minimum values of C_e are obtained. The critical value of the capacitor is selected such that the maximum power can be obtained from the generator output. The wind turbine is modeled using the mechanical power equation,

$$P_m = 0.5\rho A C_p v^3{}_w \quad (1)$$

Where, ρ is the air density (kg/m^3), A is the turbine swept area, C_p is the performance coefficient of the turbine, and $v^3{}_w$ is the wind velocity.

The mechanical power is derived using the performance coefficient which is related to the blade theory and the turbine design. The blade theory gives the relation between the Tip Speed Ratio (TSR) which is given as,

$$C_p = 0.22(116\lambda_i - 0.4\beta - 5)e^{-12.5\lambda_i} \quad (2)$$

$$\lambda_i = \frac{1}{\lambda + 0.08\beta} - \frac{0.035}{1+\beta^3} \quad (3)$$

Where: β is the pitch angle (degree) and λ is the TSR which is given by, $\lambda = \omega_m R/V_w$. From this the mechanical torque is given as,

$$T_m = P_m/\omega_m \quad (4)$$

Where ω_m is the rotor angular speed (rad/sec)

The modeling is generally based on the d-q axis equations which is generally represented as in the form of Matrix,

$$\frac{d}{dt}\begin{bmatrix} i^e_{ds} \\ i^e_{qs} \end{bmatrix} = \begin{bmatrix} \frac{-R_s}{L_d} & \frac{-L_d P\omega_m}{L_d} \\ \frac{-L_d P\omega_m}{L_q} & \frac{-R_s}{L_q} \end{bmatrix} \begin{bmatrix} i^e_{ds} \\ i^e_{qs} \end{bmatrix} - \begin{bmatrix} V^e_{ds} \\ \frac{V^e_{qs} - P\omega\psi_{pm}}{L_q} \end{bmatrix} \quad (5)$$

Where

i^e_{ds} and i^e_{ds} are the Stator direct and quadrature current components respectively,

V^e_{ds} and V^e_{qs} are the direct and the quadrature voltage components respectively,

R_s is thestator resistance, L_d and L_q are the direct and quadrature inductance respectively, P is the number of pole pairs, and ψ_{pm} is the magnetic flux (weber)

The electromagnetic torque is given by,

$$T_e = {}^3/_2 \mathrm{P}\left(i^e_{qs}\psi_{pm} + (L_d - L_q) i^e_{qs} i^e_{ds}\right) \quad (6)$$

From the mechanical equation the electromechanical torque equation is given as,

$$T_m - T_e = \mathrm{J}d\omega_m/dt + \mathrm{B}\omega_m \quad (7)$$

Where J is the inertia of the machine and B is the friction co-efficient.

The input data are used to produce the torque in the rotor reference frame. The excited power developed at the generator terminals are obtained from the d-axis and q-axis equivalent circuits are obtained as below from the figure 2,

$$r_s i_{qs} + L_s \frac{di_{qs}}{dt} + L_m \frac{di_{qr}}{dt} = V_{ds}\omega_e \quad (8)$$

$$r_r i_{qr} + L_r \frac{di_{qr}}{dt} + L_m \frac{di_{qs}}{dt} = V_{dr}(\omega_e - \omega_r) \quad (9)$$

$$r_s i_{ds} + L_s \frac{di_{ds}}{dt} + L_m \frac{di_{dr}}{dt} = -V_{ds} + V_{qs}\omega_e \quad (10)$$

$$r_r i_{qr} + L_r \frac{di_{dr}}{dt} + L_m \frac{di_{ds}}{dt} = V_{qr}(\omega_e - \omega_r) \quad (11)$$

The dynamics of the self-excited induction generator can be represented by the following electromechanical equations derived in the synchronously rotating d-q reference frame.

$$pi_{qs} = -K_1 r_s i_{qs} - (\omega_e + K_1 L_m \omega_r) i_{ds} + K_2 r_r i_{qr} - K_1 L_m \omega_r i_{dr} \quad (12)$$

$$pi_{ds} = -K_1 r_s i_{ds} - (\omega_e + K_2 L_m \omega_r) i_{qs} + K_2 r_r i_{dr} - K_1 L_m \omega_r i_{qr} - K_1 V_{ds} \quad (13)$$

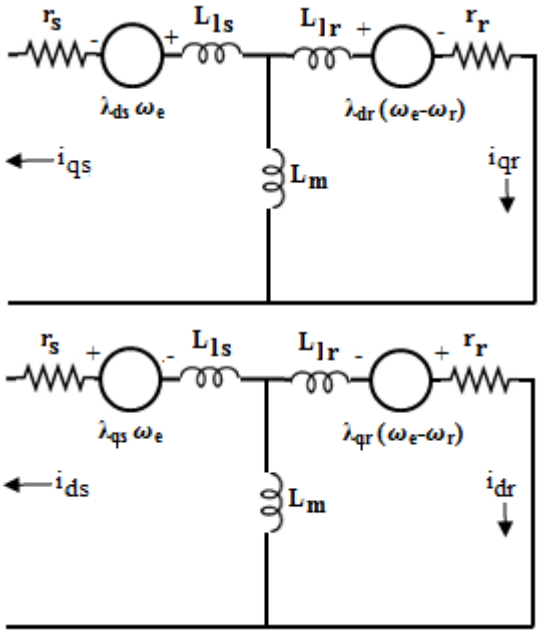

Figure 2. Equivalent circuits of SEIG in d-q reference frame

$$pi_{qr} = K_2 L_s \omega_r i_{ds} + K_2 r_s i_{qs} + (K_1 L_s \omega_r - \omega_e) i_{dr} + [(r_r + K_2 L_m r_r] i_{qr} \quad (14)$$

$$pi_{dr} = K_2 L_s \omega_r i_{qs} + K_2 r_s i_{ds} + (K_1 L_s \omega_r - \omega_e) i_{qr} + [(r_r + K_2 L_m r_r)/L_r] i_{dr} + K_2 V_{ds} \quad (15)$$

$$pV_{ds} = \frac{i_{dc}}{c},\ \omega_e = \frac{i_{qc}}{CV_{ds}} \tag{16}$$

where$K_1 = \frac{L_r}{L_S L_r - L_m^2}$ *and* $K_2 = \frac{L_m}{L_S L_r - L_m^2}$

Equations (12) - (16) are derived assuming that the d-axis is aligned with the stator terminal voltage phasor (i.e. V_{qs} = 0). In self-excited induction generators, the magnitude of the generated air-gap voltage in the steady state equation is given by,

$$V_g = \omega_e L_m |i_m| \tag{17}$$

Where,

$$|i_m| = \sqrt{(i_{qs} + i_{qr})^2 + (i_{ds} + i_{dr})^2} \tag{18}$$

$L_m = f(i_m)$

The electromagnetic torque T_g developed by the induction generator is expressed as,

$$T_g = -1.5\left(\frac{Poles}{2}\right) L_m\left(i_{qs} i_{dr} - i_{ds} i_{qr}\right) \tag{19}$$

The wind turbine and induction generator rotors are represented as a lumped mass. So the dynamic equation of motion is written as,

$$p\omega_r = \left((T_t / G_r) - T_g\right) / J_g \tag{20}$$

The developed electromagnetic torque and the torque balance equations are,

$$T_e = \left(\frac{3}{2}\right)\left(\frac{P}{2}\right) L_m\left(i_{dr} i_{qs} - i_{qr} i_{ds}\right) \tag{21}$$

$$T_{shaft} = T_e + J\left(\frac{P}{2}\right) p\omega_r \tag{22}$$

The torque balance equation is expressed in speed derivative form as,

$$p\omega_r = \left(\frac{P}{2J}\right)\left(T_e - T_{shaft}\right) \tag{23}$$

3. Modeling of Impedance Source Inverter

A three phase Impedance Source Inverter (ZSI) has replaced conventional type inverters which has shoot though limitations. The Z-Source network consists of two capacitors (C_1 and C_2) and two inductors (L_1 and L_2) connected in 'Z' shape. This network eliminates the shoot-through limitations by supplying equivalent voltage level. The modeling of the Z-source can be explained from the figure 3. The z-source components are assumed to have internal resistance value which is not shown in the figure as it is practically understood. Let us consider the values of the internal resistance for the inductor L_1 and L_2 as r_{L1} and r_{L2} respectively. Similarly, the internal resistance of the capacitors C_1 and C_2 are r_{C1} and r_{C2} respectively.

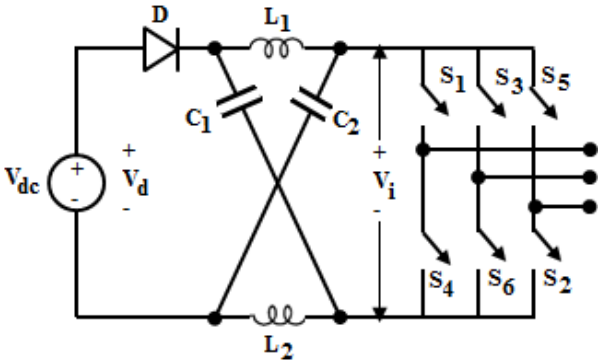

Figure 3. Impedance Source Inverter (ZSI)

The values of the two inductors and is supplied to the inverter supply.
$L_1 = L_2 = L$; $C_1 = C_2 = C$; understandably,
$r_{L1} = r_{L2} = r_L$ and $r_{C1} = r_{C2} = r_C$

During the shoot through period in the inverter, switches in any one of the legs is turned on and the voltage across the load falls to zero until the shoot through time is crossed. This probably happens during every cycle. This can be mathematically represented using matrix expression as shown.

$$\begin{bmatrix} L\frac{di_{L1}}{dt} \\ L\frac{di_{L2}}{dt} \\ C\frac{dv_{C1}}{dt} \\ C\frac{dv_{C2}}{dt} \end{bmatrix} = \begin{bmatrix} -(r_C + r_L) & 0 & 1 & 0 \\ 0 & -(r_C + r_L) & 0 & 1 \\ 0 & -1 & 0 & 0 \\ -1 & 0 & 0 & 0 \end{bmatrix} \begin{bmatrix} i_{L1} \\ i_{L2} \\ v_{C1} \\ v_{C2} \end{bmatrix}$$

During zero shoot through state, the source charges the Z-source capacitors through the inductors. Thus the state averaging equations are can be formed from the matrix,

$$\begin{bmatrix} L\frac{di_{L1}}{dt} \\ L\frac{di_{L2}}{dt} \\ C\frac{dv_{C1}}{dt} \\ C\frac{dv_{C2}}{dt} \end{bmatrix} = \begin{bmatrix} -(r_C + r_L) & 0 & 1 & 0 \\ 0 & -(r_C + r_L) & 0 & 1 \\ 0 & -1 & 0 & 0 \\ -1 & 0 & 0 & 0 \end{bmatrix} \begin{bmatrix} i_{L1} \\ i_{L2} \\ v_{C1} \\ v_{C2} \end{bmatrix} + \begin{bmatrix} 1 & r_C \\ 1 & r_C \\ 0 & -1 \\ 0 & -1 \end{bmatrix} \begin{bmatrix} V_{dc} \\ i_{ac} \end{bmatrix}$$

Let,

$V_{c1} = V_{c2} = V_c$ (24)

$V_{L1} = V_{L2} = V_L$ (25)

Also, $V_L = V_c$; $V_D = 2V_c$; $V_i = 0$
During the switching cycle T

$V_L = V_{dc} - V_c$ (26)

$V_d = V_{dc}; V_i = V_c - V_L = 2\,V_c - V_{dc}$
$V_i = 2V_c - V_{dc}$ (27)

$T = T_o + T_1$ (28)

The average voltage of the inductors over one switching period (T) should be zero in steady state,

$V_L = T_o * V_c + T_1 (V_{dc} - V_c) / T = 0;\ V_L = (T_o * V_c + V_{dc} * T_1 - V_c * T_1) / T = 0$
$V_L = (T_o - T_1)\, V_C / T + (T_1 * V_o) / T$
$V_c / V_{dc} = T_1 / (T_1 - T_o)$ (29)

Similarly the average DC link voltage across the inverter bridge can be found as follows from Equation (28)

$V_i = (T_o * 0 + T_1) * (2V_c - V_{dc}) / T$ (30)

$V_i = (2V_c.\ T_1/T) - (T_1 V_{dc}/T);\ 2V_c = V_{dc}$

From Equation (29)

$T_1 * V_{dc} / (T_1 - T_o) = 2V_c * T_1 / (T_1 - T_o);\ V_c = V_{dc} * T_1 / (T_1 - T_o)$

The peak DC link voltage across the inverter bridge is

$V_i = V_c - V_L = 2\,V_c - V_{dc} \quad = T / (T_1 - T_o).V_{dc} = B * V_{dc}$

Where $B = T / (T_1 - T_0)$ i.e≥ 1 (31)

B is a boost factor

The Z-sources voltage is then inverted by the three phase inverter circuit. The inverter circuit is operated using the PWM techniques. The PWM techniques have its own special features based on the application. The proposed work for any industrial application should operate at minimum harmonic levels. The selection of PWM techniques is performed and analyzed.

4. Topology of PWM Inverters

The PWM refers to modeling of the switch operation techniques to control the power supply applied to any converter switches. The conversion of DC to AC source performed by an inverter circuit is basically involving the switching techniques. The PWM is generated by comparing two wave signals such that one of them is a carried waveform. The carrier waveform can generally be triangular waveform and the reference signal can be either square or trapezoidal or sinusoidal waveforms. The proposed ZSI is performed on different PWM techniques operating at 10 kHz switching frequency and the result is compared.

A. Modeling of Trapezoidal PWM Technique

The triangular carrier wave is compared with the modulated trapezoidal wave. The trapezoidal waveform is generated whose amplitude is limited to the amplitude of the carrier triangular waveform ($+A_r$ and $-A_r$). The trapezoidal pulse width modulation (TPWM) is shown in the figure 4. The peak value is however given by A_{rmax}. The relationship between these values as shown in the figure 4a is given by,

$A_r = \sigma\, A_{rmax}$ (32)

Where, σ is the triangular factor.

B. Modeling of Sinusoidal PWM Technique

Sinusoidal Pulse Width Modulation is one of the most common techniques applied in an inverter for the AC output. The modeling is much similar to the previous PWM technique where the signal waveform here is a sinusoidal waveform. The modulation obtained at various stages is more effective compared to TPWM. The pulses near the edges of the half cycle are always narrower than the pulses near the center of the half cycle. To change the effective output voltage, the widths of all pulses are increased or decreased while maintaining the sinusoidal proportionality. The pulse width is proportionate with the sine wave amplitude. The gating pulses are generated and are applied for the switching sequences such that the output voltage,

$V_{out} = V_i\sqrt{\frac{p\delta}{\pi}}$ Where, p is the number of pulses, δ is the pulse width. The generation of SPWM is shown in the figure 4b.

C. Modeling of Space Vector PWM Technique

The Space vector modulation (SVM) is an algorithm designed for the three phase inverters for the pulse generation. The main advantage of this control technique is, compared to other PWM techniques the output distortion is minimized and implemented to save the power losses. The SVPWM technique follows the vector model of source which is modulated to generate the pulses for different switching stages separate. The three phase system defined by ax(t), ay(t) az(t) can be represented uniquely by a rotating vector as ,

$$a_s = \frac{2}{3}\left[a_x(t) + a.a_Y(t) + a^2.a_Z(t)\right] \quad (33)$$

Given a three-phase system, the vector representation is achieved by the following 3/2 transformation:

$$\begin{bmatrix} A_\alpha \\ A_\beta \end{bmatrix} = \frac{2}{3}.\begin{bmatrix} 1 & \frac{-1}{2} & \frac{-1}{2} \\ 0 & \frac{\sqrt{3}}{2} & \frac{-\sqrt{3}}{2} \end{bmatrix}.\begin{bmatrix} a_X \\ a_Y \\ a_Z \end{bmatrix}$$

Where (Aα, Aβ) are forming an orthogonal 2-phase system and $a_S = A_\alpha + jA_\beta$. A vector can be uniquely defined in the complex plane by these components. The reverse transformation (2/3 Transformation) is given by,

$$a_X(t) = Re[a_S] + a_0(t);\ a_Y(t) = Re[a^2.a_s] + a_0(t);\ a_Z(t) = Re[a.a_s] + a_0(t); \quad (34)$$

$$a_0 = \frac{1}{3}.[a_X(t) + a_Y(t) + a_Z(t)]$$

The switching time periods for the six sector equivalent to three phase outputs as in figure 4c are obtained and given as,

$S_{V0} = T_{S4}T_{S6}T_{S2}$;$S_{V1} = T_{S1}T_{S6}T_{S2}$; $S_{V2} = T_{S1}T_{S3}T_{S2}$;$S_{V3} = T_{S4}T_{S3}T_{S2}$;
$S_{V4} = T_{S4}T_{S3}T_{S5}S_{V5} = T_{S4}T_{S6}T_{S5}$;$S_{V6} = T_{S1}T_{S6}T_{S5}$;$S_{V7} = T_{S1}T_{S3}T_{S5}$

Where T is the switching time period such that T_{Sn} for n = 1, 2, 3, …6.

The switching stages represents the seven stages constituting five active stages and two zero stages. The output is obtained for all the active stages but during the zero stage the output is zero. The impedance sources supply the power to the output during the zero stages thus contributing the continuous power at the output.

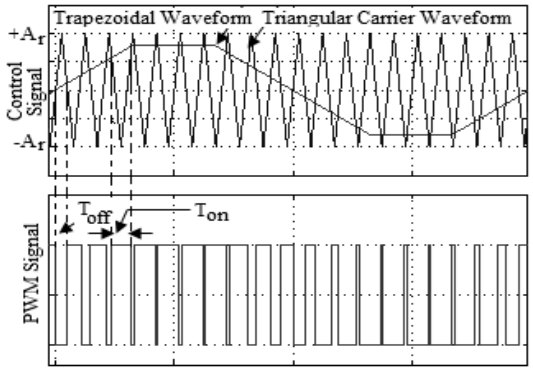

(a)

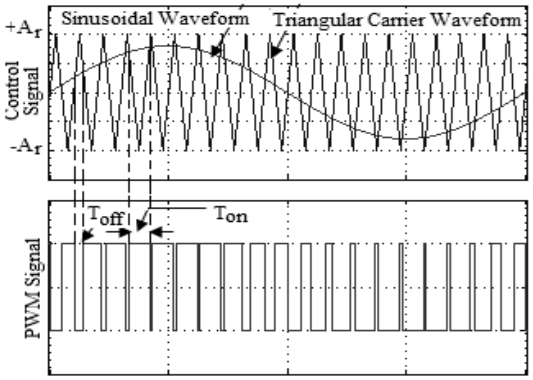

(b)

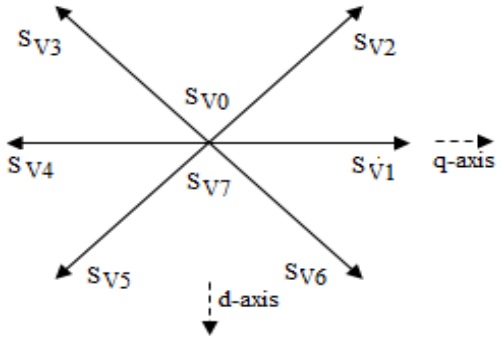

(c)

Figure 4. PWM Techniques (a) Trapezoidal PWM (b) Sinusoidal PWM (c) Space Vector d-q axis locations and switching sequence

5. Simulation Verification

The wind driven SEIG is modeled for 900W and the results obtained are shown in figure 5. The figure 5a, shows the output RMS values of the voltage and the current obtained from a 900W wind turbine during the wind velocity of 11m/s. The RMS voltage of V_{rms} is recorded as 240V and the RMS current is recorded to be 4.2A. The constant voltage and current obtained have high level of distorted vales with average of 20V and 0.1A respectively. The solution to the harmonic indices recorded is eliminated at different levels using the proposed PWM techniques. The figure 5b, shows the rotor speed and turbine power respectively. It is note that

the values of the rotor speed and the power for the given parameter are N_r=2250rpm and P_g=900W. The output from SEIG is rectified and the rectified DC voltage obtained is 150V. The above said harmonic distortions are eliminated to a level using the PWW techniques proposed. The figure 5d, shows the comparison of the three phase wind turbine and the SVPWM switched three phase inverter output. It is noted form the figure that the required constant inverter terminal RMS voltage and RMS current as V_{0rms}=175V and I_{0rms}=4.0A respectively. It is also observed that voltage and current distortions are much less. In a drive application it is more necessary to work on the Total Current Harmonic Distortions (THD_i). The results for the TPWM, SPWM and SVPWM are situated and shown in the figure 6 and the THD_i is tabulated in the table 1.

Table I. THDi Comparison of Simulated Model

PWM Techniques	THD_i at m=0.8
Trapezoidal PWM	25.50%
Sinusoidal PWM	10.60%
Space Vector PWM	4.17%

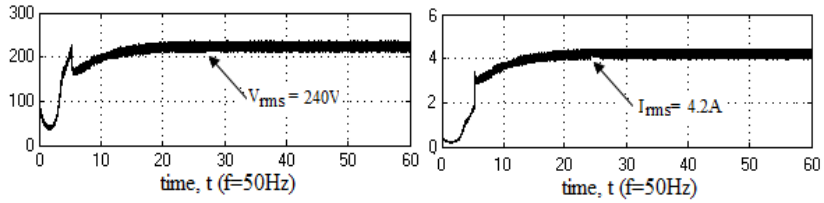

(a)

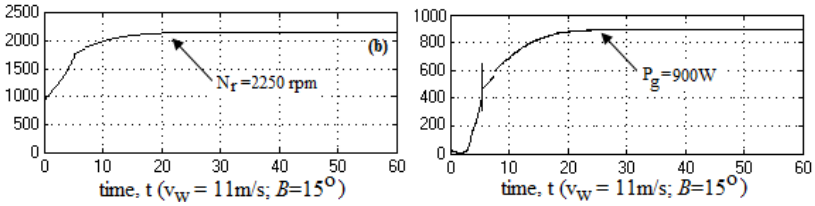

(b)

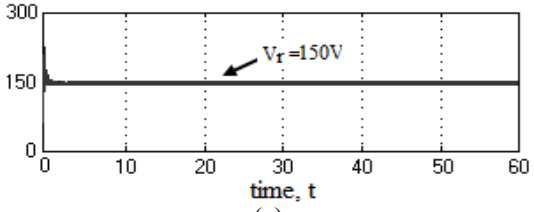

(c)

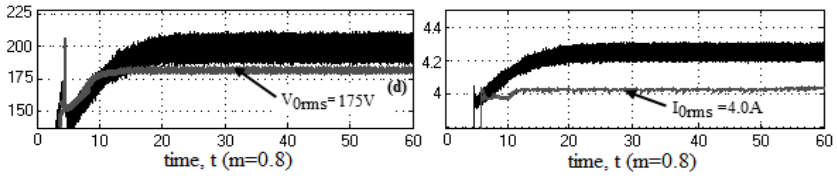

(d)

Figure 5. Proposed System Simulation Result (a) wind turbine voltage and outputs (b) wind turbine speed and power outputs (c) rectified DC voltage (d) inverter output using SVPWM at 10 kHz

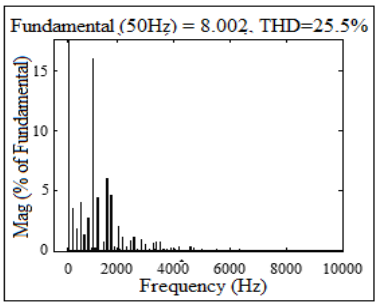

(a)

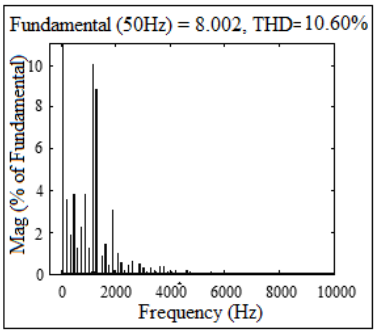

(b)

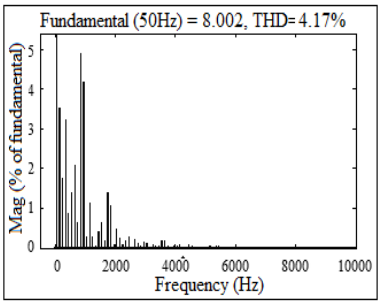

(c)

Figure 6. THD_i (a) using TPWM (b) using SPWM (c) using SVPWM

6. Experimental Verification

The evaluation of the harmonic levels in simulation modeling shows the implementation of SVPWM for a drive application is well effective. However to verify the simulation setup, a similar 900W prototype model of the proposed system using the Space Vector Pulse Width

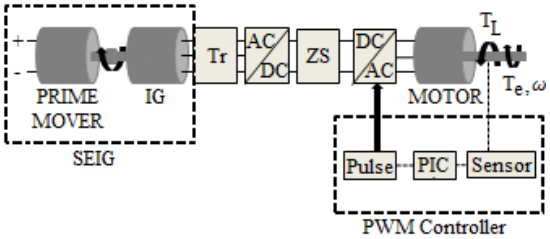

Figure 7. Experimental model of the prototype model

Modulation (SVPWM) is experimented. The wind driven SEIG is modeled by driving the SEIG by connecting to a DC motor as a prime mover. The wind speed is characterized by the resistor control of DC motor. The experimental model is shown in the figure 7.

The three SEIG output is measured is practically stepped down using a step down transformed to obtain a low voltage outputs. The hardware results obtained are shown in the figure 8.

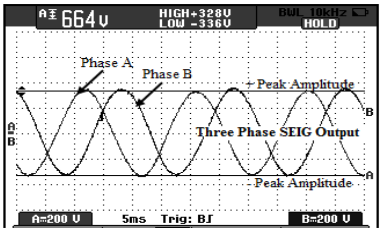

(a)

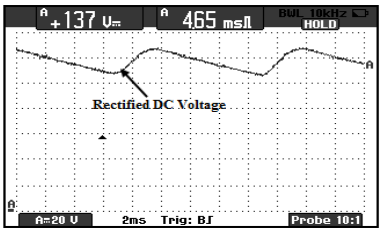

(b)

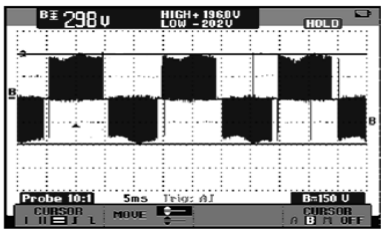

(c)

Figure 8. Hardware results (a) SEIG output voltage (b) Rectified DC voltage (c) ZSI output voltage for f_{sw}=10 kHz.

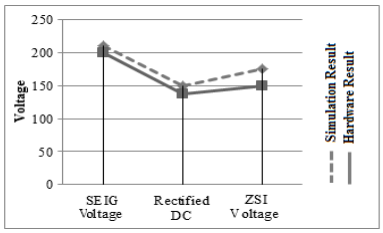

Figure 9. Comparison of Simulation and Hardware Results

The voltage RMS obtained to be 200V. This AC voltage is rectified using a three phase diode bridge rectifier. The uncontrolled rectified DC voltage obtained is 137V. The DC output of the SEIG is supplied to a three phase ZSI. The single phase ZSI is used to operate at 10 kHz switching frequency. The SPWM switching pulses as found to be low from the simulated result is implemented in the hardware prototype model and is programed using PIC controller. The

output of the three phases ZSI is measured for the phase B is obtained to be obtained to be 150V. The results obtained for a 900W proposed model for both simulation and hardware implementation is compared and shown in the figure 9. It is observed that in this 900W system, the simulation and the hardware values of the SEIG outputs are 240V and 200V respectively, the rectified DC outputs are 150V and 137V respectively and the ZSI voltages are 175V and 150V respectively. The system results in a low harmonic level when a three phase ZSI is controlled using the SVPWM technique is analyzed.

The input parameters used for the proposed system is tabulated in the table 2.

Table 2. Parameter Values Used

Symbols	Description	Values
V_w	Wind velocity	11 m/s
R	Rotor radius	2 m.
β	Blade pitch angle	15^0
Gr	Gear ratio	1:30
$L_1=L_2=L$	Z-Source inductance	1500mH
$C_1=C_2=C$	Z-Source capacitance	150μF
C_e	Excitation capacitance	55μF
T_L	Load torque	78N-m
f_{sw}	Switching frequency	10 kHz
M	Modulation Index	0.8
f_c	Carrier frequency	3 kHz
f_r	Reference frequency	50Hz
f	System frequency	50 Hz
T_r	Transformer	380V/210V

7. Conclusion

The wide range of industrial drive application inhibits on the harmonic distortion levels causing the power loss for very high voltage applications. The three phase induction motor drive used in the proposed work is controlled using a PWM inverter specially designed to eliminate shoot through problems however referred as ZSI. The three types of switching techniques, trapezoidal PWM, Sinusoidal PWM and Space Vector PWM are modeled and the total harmonic distortions are obtained. The modeling of wind driven Self-Excited Induction Generator (SEIG) is practically analytical to a DC motor used as a prime mover to a SEIG. The THD_i of the techniques involved shows the implementation of SVPWM for the induction motor drives saves 16% power loss compared to other PWM techniques thus increasing the performance of the motor drives. A similar system model is developed for a 900W prototype model with a three phase ZSI controlled using SVPWM. Comparative analysis between the simulation and hardware results shows that a three phase ZSI controlled using SVPWM is in effective with an industrial drive application for the Wind Energy Conversion System.

References

[1] Hau Geng, Xu D, Bin Wu and Wei Huang, "Experimental Investigation of Steady State and transient performance of a self-excited induction generator", *IET Generation, Transmission and Distribution,* vol.5, issue 12, pp.1233-1239, Dec 2011.

[2] R. Karthigaivel, N Kumeresan and Subbiah M, "Analysis and Control of self-excited induction generator-converter system for battery charging applications", *IET Electric Power Applications,* vol.5, issue 2, pp.247-257, Feb 2011.
[3] Amin M.M and O.A. Mohammed, "Development of High-performance Grid connected wind energy conversion system for optimum utilization of variable speed wind turbines", *IEEE Transactions on Sustainable Energy,* vol. 2, issue 3, pp.235-245, June 2011.
[4] M. Bodson and O. Kiselychnyk, "Analysis of triggered Self-Excited Induction Generators and Experimental Validation", *IEEE Transactions on Energy Conversion,* vol.27, issue 2, pp.238-249, Jun 2012
[5] M Nagpal, TG Martinich, A Bimbhra and M Ramamurthy, "Hazardous Temporary Over voltages from Self-Excited large Induction Motors", *IEEE Transactions on Power Delivery,* vol.27, issue 4, pp.2098-2104, Oct 2012.
[6] S. S. Murthy, B Singh, Sandeep V, "A Novel and Comprehensive Performance Analysis of a Single-Phase Two Winding Self-Excited Induction Generator", *IEEE Transactions on Energy Conversion,* vol.27, issue 1, pp.117-127, Feb 2012.
[7] Yu Tang, Shaojun Xie, Jiudong Ding, "Pulsewidth Modulation of Z-Source Inverter with Minimum Current Ripple", *IEEE Transactions on Industrial Electronics,* vol.61, Issue 1, pp. 98-106, July 2013.
[8] Zheng Zhao, Jih-Sheng Lai and Younghoon Cho, "Dual-Mode Double-Carrier-Based Sinusoidal Pulse Width Modulation Inverter with Adaptive Smooth Transition Control Between Modes", *IEEE Transactions on Industrial Electronics*, vol. 60, Issue 5, pp. 2094-2103, May 2013.
[9] Georgakas K, Safacas A, "Modified sinusoidal pulse-width modulation operation technique of an AC-AC single-phase converter to optimize the power factor, *IET Transactions on Power Electronics,* vol. 3, Issue 3, pp. 454-464, May 2010.
[10] A. C. Oliveira, C B Jacobina, AM N Lima, "Improved Dead Time Compensation for Sinusoidal PWM Inverters Operating at High Switching Frequencies", *IEEE Transactions on Industrial Electronics,* vol. 54, Issue 4, pp. 2295-2304, Aug 2007.
[11] LA de Souza Ribeiro, C B Jacobina, AMN Lima, AC Oliveira, "Real Time estimation of induction machine using sinusoidal PWM voltage waveforms", *IEEE Transactions on Industrial Applications,* vol. 36, Issue 3, pp. 743-754, June 2000.
[12] Sasikumar M. and Chenthur Pandian S., "Modeling and Analysis of Cascaded H-Bridge Inverter for Wind Driven Isolated Self – Excited Induction Generators", International *Journal on Electrical Engineering and Informatics*, Vol.3, No. 2, pp. 132-145, 2011.
[13] J. Prieto, F Barrero, MJ Duran, S Toral Marin, MA Perales, " SVM Procedure for n-phase with Low Harmonic Distortion in the Over modulation Region", *IEEE Transactions on Industrial Electronics,* vol. 61, Issue 1, pp. 92-97, Jan 2014.
[14] Qin Lei, Fang Zheng Peng, "Space Vector Pulsewidth Modulation for a Buck-Boost Voltage/Current Source Inverter, *IEEE Transactions on Power Electronics",* vol. 29, Issue 1, pp.266-274, Jan 2014.
[15] F. B. Effah, P Wheeler, J Clare and Watson A, "Space-Vector-Modulated Three Level Inverters with a single Z-Source Network", *IEEE Transactions on Power Electronics,* vol.28, Issue 6, pp. 2806-281, June 2013.
[16] Y. Lui, B Ge, H Abu-Rub and F Z Peng, "Overview of Space Vector Modulations for three phase Z-Source/Quazi-Z-source inverters", *IEEE Transaction on Power Electronics,* vol. 29, issue 4, pp.2098-2108, April 2014.
[17] K. Jia, G Bohlin, M Enohnyaket, R Thottappillil, "Modelling of an AC motor with high accuracy in a wide frequency range", *IET Power Electronics Application,* vol.7, Issue 2, pp. 116-122, Feb 2013.
[18] A. M. Bazzi, V T Buyukdegirmenci, PT Krein, "System-Level Power Loss Sensitivity to Various Control Variable in Vector-Controlled Induction Motor Drives", *IEEE Transaction on Industry Applications,* vol. 49, Issue 3, pp. 1367-1373, June 2013.

[19] A. Smith, S Gadoue, M Armstrong, J Finch, “Improved Method for scalar control of induction motor drives”, *IET Electric Power Applications,* vol. 7, Issue 6, pp.487-498, July 2013.
[20] Sangshin Kwak, H A Toliyat, “Hybrid Solutions for load commutated inverter fed induction motor drives”, *IEEE Transactions on industry Applications,* vol. 41, Issue 1, pp.83-90, Feb 2005.
[21] Sangshin Kwak, HA Toliyat, “A Hybrid Converter for High-Performance Large Induction Motor Drives”, *IEEE Transactions on Energy Conversion,”* vol. 20, Issue 3, pp. 504-511, Sep 2005.

Max Savio was born in Hyderabad, India in 1986. He has received Bachelor of engineering in Electrical and Electronics and Master of Engineering in Power Electronics and Drives from Jeppiaar Engineering College, Chennai, India in 2007 and 2013 respectively. He has four years of experience in industry working under electrical erection and maintenance. He is currently working as Assistant Professor in the department of Electrical and Electronics Engineering with Jeppiaar Institute of Technology, Chennai, India. He has published his works in National and International Journals. His research work involves renewable hybrid energy, power converters, PWM techniques, drives and control.

Sasikumar Murugesan has received the Bachelor degree in Electrical and Electronics Engineering from K.S.Rangasamy College of Technology, Madras University, India in 1999, and the M.Tech degree in power electronics from VIT University, in 2006. He has obtained his Ph.D. degree from Sathyabama University, Chennai in 2011. Currently he is working as a Professor and Head in Jeppiaar Engineering College, Chennai Tamilnadu, India. His area of interest includes in the fields of wind energy systems, Hybrid systems and power converter and soft-switching techniques. He is a life member of ISTE.